Journal of Engineering Science and Technology
Vol. 17, No. 4 (2022) 2431 - 2446

NONLINEAR NEURAL PID CONTROLLER FOR DEPRESSING FLUCTUATION OF CURVED BEAM SUBJECTED TO DIFFERENT LOAD CONDITIONS

WAJDI SADIK ABOUD[1,*],
HAYDER SABAH ABD AL-AMIR[2], HAMEED SHAMKHI JABER[2]

[1]Prosthetics and Orthotics Engineering Department, Faculty of engineering, Al-Nahrain University, Baghdad, Iraq
[2]Power Mechanics Department, Institute of Technology - Baghdad, Middle Technical University, Baghdad, Iraq
*Corresponding Author: wajdisadik@gmail.com

Abstract

Nowadays, many solutions have been suggested to reduce the beam deflections and failure rates due to the load applied in these beams. One of the introduced solutions was to provide effective controllers (robust controllers) that are capable of suppressing the vibration. The main contribution of this study is to derive the mathematical model for a simply supported curved beam that can be solved analytically and to be compatible with the optimal controller to minimize the beam deflections. A simply supported, in-plane, and curved beam structure with adopting different subtended angles is studied. A variable horizontal moving load and a variable vertical fluctuated load were applied to generate the vibrations. Based on the Lagrangian mechanics, the mathematical model was derived and solved analytically. Then a compatible controller was designed, and the design procedure required two stages. The Nonlinear Neural Proportional Integral Derivative (NLNPID) controller was proposed as the first stage to depress the induced vibration. In the second stage, the NLNPID parameters were tuned optimally by adopting the Particle Swarm Optimization (PSO) technique to reduce the deflections as much as possible. The controlled system was examined when the assembly was subjected to different ranges of load velocities, frequencies, and subtended angles. The results of the critical beam resonance frequency, as well as the uncertainties, were also considered. The deflections' values at the midpoint for the curved beam system with and without controlling were compared. The results show that the deflections of the curved beam were improved up to 97.7% in the case of using the NLNPID controller and up to 56.4 % in the case of using the classical PID controller. The simulation results demonstrated the significant ability of the proposed controller to dampen the beam's deflections at various subtended angles and load conditions.

Keywords: Curved beam, Dynamic load, Optimal PID, PSO, Robust nonlinear neural network

1. Introduction

It is becoming increasingly difficult to ignore the structural issues that are subject to dynamic loads and changes with time. Engineering designers of this field became so worried about these issues because these loads generate vibrations that might be unexpected in the structure, especially with the increasing life of the structures, where some of their properties might change or cracks might appear leading to changes in their resonance frequencies. The dynamic loads greatly affect and accelerate crack spreading, which means shortening the life of the structure. Many research works in the literature deal with modelling and solving different physical and engineering applications using numerical approaches, such as finite elements.

On the other hand, there were massive studies that deal with analytical modelling based on analytical solutions such as Newtonian and Lagrangian mechanics to solve the same applications [1-6]. Hence, the interest in the analytical studies of the dynamic loads' effect on the behaviour of the structure is crucial and trying to develop techniques to control these vibrations to reduce the bad effect is important as well. Generally, the curved beam has many applications in various engineering fields, such as cranes, turbine blades, thin-wall cylinders, bridge design, and pipes. In the current interesting studies, the main applications of curved beam structures are concerning bridge design and transporting pipes of fluid [7-10].

A considerable amount of works in the literature on the development of a plane and a curved beam element exists and continues to grow [11-16]. Some of them focused on nature shape function and the vibrations induced. Others focused on proposed controllers of displacement reductions. Some of these research works are given herein. Shanmugam et al. [17] examined the failure mode in a steel beam curved in a plane when the mid-span was loaded by concentrating loads. The study examined two groups of horizontally curved girders. Izzet and Mohammed [18] conducted an experimental program to analyse the flexural response of a composite curve beam with I-girder decks. The experiment consisted of testing five models by subjecting loads according to the Iraqi Standard Bridge live. The main obtained results showed that when the curvature increases, the deflection and the longitudinal girder strains increase, while the girder spacing exerted only a very small influence. Boğa and Onur [19] performed analytical and numerical axial stress analysis for a functionally graded beam (FGB) under thermal loading. The properties of FGBs were varied. The effect of these variations was investigated. Yanze et al. [20] studied theoretical and experimental analysis of curved beams related to a thin-walled structure. The normal finite element analysis was used as the static analytical method. The results were verified by an experimental method based on the one-dimensional deformation theory.

Additionally, controlling of the beams' structures is still the main subject of many research works, where Khot et al. [21] adopted the cantilever beam in a reduced model representation to apply an optimal controller. The study proposed the Linear Quadratic Regulator (LQR) algorithm based on the state feedback control law. Khot et al. [22] studied the extraction of the full and reduced mathematical models of a cantilever beam from its finite element (FE) model using MATLAB. For this model, a design of a proportional-integral-derivative (PID) controller with the output feedback theory was proposed.

Abdelhafez and Nassar [23] investigated the effects of the loop delays in the feedback controller that was used in the forced and self-excited nonlinear beam

structure. The study used the multiple timescales perturbation techniques to obtain a first-order approximate solution. Then, the time delay for such a controller was studied. For validation purposes, the analytical and numerical results were compared in the study. Moreover, Abiduan et al. [24] presented the design and implementation of a PID controller for the dynamic behaviour of a fixed-fixed beam. The beam was subjected to a dynamic load and rested on a nonlinear vibration isolator at the middle point. Based on the pole placement technique, optimal gains were obtained providing a significant reduction in the beam deflection.

More recently, Zhang and Li [25] used a decoupling technique based on adaptive control for modal vibrations of a smart flexible beam with two piezoelectric patches. A multivariable minimum variance self-tuning control was used for designing the proposed control law. The theoretical and experimental results showed efficient overturning vibrations for a smart flexible beam. Moreover, Singh et al. [26] adopted the poling tuned piezoelectric actuator method as an active vibration control of a smart cantilever beam. The vibrating response of the piezo-laminated cantilever beam was modelled using a lumped parameter approach. The fuzzy logic controller was then used to control the vibration, where 49 rules have been established to develop the controller.

Based on the previously mentioned studies, most reported works demonstrated a lack of a deeply detailed technique to merge the deflection responses with the control law analytically for the beam structure problems and the studies focused only on numerical results. Therefore, the main contribution of this work is to present simplified analytical modelling and a solution strategy that can be used as an initial stage in designing a controller for beam structures, in which the parameters of the controller are specified to identify the actual actuator power ability. Later on, this power of actuation can be adopted in the designed controller for the curved beam system as real and reliable power.

It is worth noticing that in other numerical modelling analyses of the curved beams in the literature, such as the finite element method, it is very difficult to design a controller for the beam model. In addition, long-time executing processes and very fast computers are required. However, the current strategy is characterized by presenting a solvable model for the curved beam problem when subjected to a moving load with fluctuated amplitude values in a simplified and easy-to-handle approach. Therefore, the problem of the curved beam in this study is not only simplified to the second ordinary differential equation (2nd ODE) but also the ability to design a trouble-free controller is gained by directly connecting the beam governing equation with the control law of the controller. In other words, the simulation process of such a model is facile handled, fast, and does not require high computer processing levels.

This study aims at modelling and analysing a curved beam subjected to different dynamic loads. Furthermore, the beam deflection is minimized by proposing an optimal PID controller that can be tuned by the PSO algorithm to provide optimal gains through which the beam deflections are minimized along the whole beam length. Besides, a robust controller is also considered to overcome parameter uncertainties.

The paper has been organized in the following way. In Section 2, the derivation of the mathematical model for the curved beam is presented by introducing all the assumptions and the important boundary conditions. The proposed nonlinear controller and the optimal procedure for selecting the optimum controller gains are given in

Section 3. In addition, the section discusses the design of the controller based on the particle swarm optimization (PSO) algorithm. In Section 4, the simulation results of the controlled system are presented and discussed. Finally, the paper is closed by pointing out the main conclusions and suggestions for future works in Section 5.

2. Modelling of the Curved Beam

In this study, the simply supported vertical curved beam is considered, as shown in Fig. 1, in which (θ) denotes the subtended angle, (R) is the radius of curvature, and (L) is the length of the beam. The coordinate system adopted is right-handed, where the x-axis is tangent to the centroidal axis of the beam, and the y and z axes coincide with the principal axis of the cross-section. The model of the curved beam has two dependent variables; displacement in the x-axis $u(x, t)$ and displacement in the z-axis $w(x, t)$, where the x-axis is tangent to the centroidal axis of the beam.

Moreover, the following assumptions were considered to formulate and simplify the interesting case study [15];

- For the possibility of using linear theory, all the deformations are assumed small, and the materials are elastic.
- The curved beam has a constant material density.
- The curved beam's cross-sections and its second moment of area are constant.
- The warping resistance was ignored.

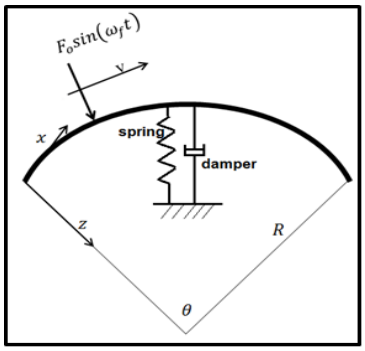

Fig. 1. A schematic diagram of the curved beam subjected to a harmonic moving load.

In addition, a moving and fluctuating load is assumed as the applied load on the curved beam. A spring damper system is used as a vibration isolator in the middle of the curved beam. Based on the differences between kinetic and potential energies, which denote the Lagrange concept, the equation of motion for the interesting study was derived [4]. Specifically, the Lagrange concept with applying the assumed-mode method is adopted as follows:

The kinetic energy (KE) of the beam can be written as [27]:

$$KE = \frac{1}{2}\rho A \int_0^L \dot{w}(x,t)^2\, dx + \frac{1}{2}\rho A \int_0^L \dot{u}(x,t)^2\, dx \quad (1)$$

The potential energy (PE) of the system and the damping energy (DE) can be written as follows:

$$PE = \frac{1}{2}EA\int_0^L [u' + \frac{w}{R}]^2\,dx + \frac{1}{2}EI\int_0^L [w^{"} + \frac{w}{R^2}]^2\,dx + \frac{1}{2}kw(\frac{L}{2},t)^2 \quad (2)$$

$$DE = \frac{1}{2}c\dot{w}(\frac{L}{2},t)^2 \quad (3)$$

The displacements of the curved bean can be assumed to be of the form:

$$w(x,t) = \sum_1^\infty \psi_i(x)q_i\,(t),$$

$$u(x,t) = \sum_1^\infty \phi_i(x)p_i(t), \quad (4)$$

where (q_i) and (p_i) are generalized coordinates, and (ψ_i) and (ϕ_i) are the admissible curved beam functions that satisfy the present beam boundary conditions and are defined as follows [13]:

$$\psi_i(x) = \sin\left(\frac{i\pi x}{L}\right)$$

$$\phi_i = \frac{1}{R}\left(\frac{L}{i\pi}\right)\left\{1 - \cos\left(\frac{i\pi x}{L}\right) - [1-(-1)^i]\frac{x}{L}\right\} \quad (5)$$

Equation (5) has a different form based on the boundary conditions assumed. For this reason, new assumptions are required for other boundary conditions. In this paper, the first modes of each admissible function are taken for displacements of the curved beam, i.e.:

$$w(x,t) = \sin(\frac{\pi x}{L})q(t)$$

$$u(x,t) = \frac{1}{R}\left(\frac{L}{\pi}\right)\left\{1 - \cos\left(\frac{i\pi x}{L}\right) - [2]\frac{x}{L}\right\}p(t) \quad (6)$$

Substituting Eq. (6) into Eqs. (1), (2), and (3) and applying Lagrange's equation, the differential equation of motion for the curved beam is obtained:

$$m_{11}\ddot{p} + k_{11}p + k_{12}q = 0$$

$$m_{22}\ddot{q} + C\dot{q} + k_{21}p + (k_{22} + K)q = Qsin(\omega_f t) + u \quad (7)$$

where

$$k_{11} = EA\left[\int_0^L \frac{1}{R}\left(\frac{L}{\pi}\right)\left\{\frac{\pi}{L}\sin\left(\frac{\pi x}{L}\right) - [2]\frac{1}{L}\right\}\right]^2 dx$$

$$k_{12} = k_{21} = EA\left[\int_0^L \frac{1}{R}\left(\frac{L}{\pi}\right)\left\{\frac{\pi}{L}\sin\left(\frac{\pi x}{L}\right) - [2]\frac{1}{L}\right\}\right]\sin\left(\frac{\pi x}{L}\right)dx$$

$$k_{22} = A_1 + A_2 + A_3 + A_4$$

$$A_1 = EA\int_0^L \sin\left(\frac{\pi x}{L}\right)^2 dx$$

$$A_2 = EI\int_0^L \left[\left(\frac{\pi}{L}\right)^2 sin\left(\frac{\pi x}{L}\right)\right]^2 dx$$

$$A_3 = \frac{EI}{R^2}\int_0^L -\left(\frac{\pi}{L}\right)^2 sin\left(\frac{\pi x}{L}\right)sin\left(\frac{\pi x}{L}\right)dx$$

$$A_4 = \frac{EI}{R^4}\int_0^L sin\left(\frac{\pi x}{L}\right)sin\left(\frac{\pi x}{L}\right)dx$$

$$Q = F_o\sin(\frac{\pi X_f}{L})$$

where (Q) is a generalized force, (X_f) is the position of the moving load (F_o) along the (x) direction of the curved beam, and (u) is the control action. Table 1 illustrates the main physical parameters' values that are employed in the current calculations.

The beam physical properties are considered to be similar to those of Ref. [28] with proposing a different load amplitude, F_o.

Table 1. The parameters' values [28].

Parameter	Value	Parameter	Value
A	16×10^{-4} m^2	L	10 m
E	2×10^{14} N/m^2	ρ	8000 kg/m^3
I_y	2.133×10^{-7} m^4	First natural frequency	23.9 rad/s
F_o	500 N		

To verify the validity of the proposed model in this study, the value of the first mode frequency is calculated. The calculation shows that the first mode frequency is (114.6 rad/s) when the frequency source is (115.4 rad/s) [29]. This result is significant at the beam values of that source.

3. Nonlinear Neural PID Controller Design

3.1. Optimal PID controller

In this study, a nonlinear neural PID controller (NLNPID) is proposed. Figure 2 illustrates the schematic assembly diagram of the NLNPID controller. The PID controller structure consists of three gains, *Kp*, *Ki*, and *Kd* representing the proportional gain, the integral gain, and the derivative gain, respectively.

The particle swarm optimization (PSO) algorithm is adopted as a tuneable part for the traditional PID gains to achieve optimal gain values. Figure 3 presents the structure of the combination of the PID and PSO. In this structure, the controller consists of two parts; the first part is the direct closed-loop control for controlling the curved beam deflection at the middle position and the second part is the dynamic gains that are tuneable by the PSO algorithm to obtain optimal PID gains according to the operating conditions [30, 31].

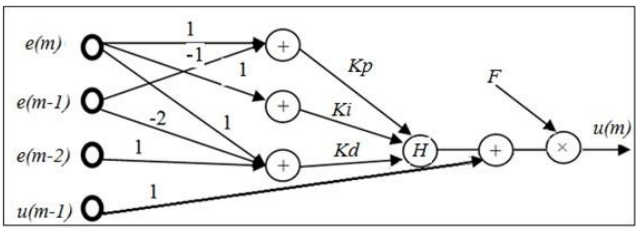

Fig. 2. The nonlinear neural PID controller architecture [30].

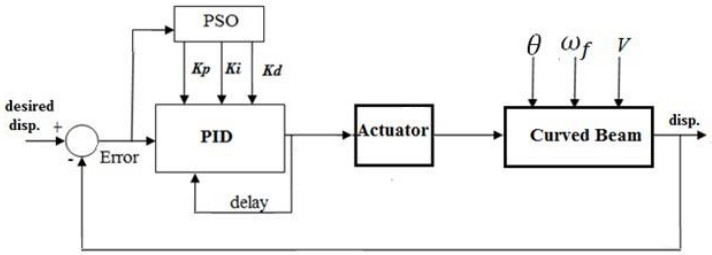

Fig. 3. The proposed controlling scheme.

The suggested control effort of the feedback flow rate NLNPID controller is expressed as:

$$u(m) = (u(m-1) + H(net)) \times F \quad (8)$$

The calculation of the weighting sum of the inputs is the first computation inside the neuron as follows [32];

$$net = K_p[e(m) - e(m-1)] + K_i e(m) + K_d[e(m) - 2e(m-1) + e(m-2)] \quad (9)$$

In the second step, the neuron output is computed according to the Polywog wavelet function as the *net* equation, as follows [32]:

$$h_n = H(net) \quad (10)$$

$$H(net) = (3(net)^2 - (net)^4)e^{-0.5(net)^2} \quad (11)$$

The input vector of the PID controller is tuned automatically and online. The vector consists of $e(m)$, $e(m\text{-}1)$, $e(m\text{-}2)$ and $u(m\text{-}1)$, where $e(m)$ denotes the input error signals and $u(m)$ denotes the output of the PID controller. In the current study, the control action, u, represents the force that acts at the middle position of the curved beam, while F represents the scaled factor. Figure 4 shows the nonlinear Polywog wavelet activation function [32], which was adopted in the construction of the currently proposed controller.

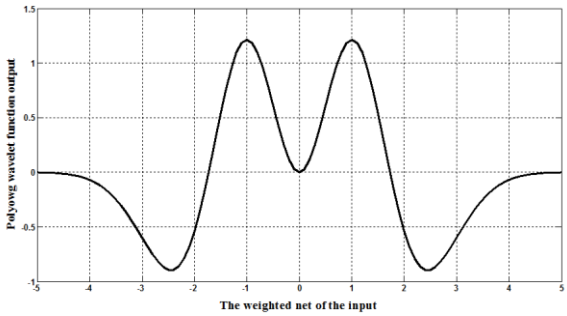

Fig. 4. The response of a nonlinear Polywog wavelet activation function [32].

3.2. Learning algorithm

The main aim of this study is to control the deflection of the curved beam by implementing the PSO algorithm for optimal online auto-tuning of the NLNPID controller. The PSO algorithm starts with an initial population of particles with random positions and velocities. The path towards the best solution (fitness) that is achieved so far is adjusted by each particle. This value is denoted as *pbest*. The path towards the best previous position attained by any member of its neighbourhood is also modified by each particle. This value is denoted as *gbest*. By an adaptive velocity, each particle moves in the search space [33].

To examine the optimal solution, the fitness function was used to evaluate the particles [34, 35].

$$V_{r,n}^{m+1} = wV_{r,n}^{m} + c_1 rand_1(pbest_{r,n}^{m} - x_{r,n}^{m}) + c_2 rand_2(gbest_{n}^{m} - x_{r,n}^{m}) \quad (12)$$

$$x_{r,n}^{m+1} = x_{r,n}^{m} + V_{r,n}^{m+1} \quad (13)$$

where $V_{r,n}^{m}$ is the velocity of the r^{th} particle at m^{th} iteration, $x_{r,n}^{m}$ is the position of the r^{th} particle at m^{th} iteration, r is the number of particles, n is the dimension of a particle, c_1 and c_2 are the acceleration constants with positive values, w is an inertial weight, $rand_1$ and $rand_2$ are random numbers between 0 and 1, $pbest_r$ is the best previous weight of the r^{th} particle, and $gbest_n$ is the best particle among all the particles in the population.

In the current analysis, $\Delta K_n^{m+1} = V_{r,n}^{m+1}$, $\Delta K_n^m = V_{r,n}^m$ and $K_n^m = x_{r,n}^m$, where K represents the parameters K_p, K_i and K_d of the NLNPID controller. The mean square error function is chosen as a criterion for estimating the model performance, as given in Eq. (14):

$$E = \frac{1}{Np}\sum_{j=1}^{Np}(disp_{desired}(m+1)^j - disp_{actual}(m+1)^j)^2, \quad (14)$$

where Np is the number of samples.

According to the basis of the PSO algorithm, a significant output response can be obtained when the value of w is from 0 to 1 and $c_1+c_2 < 4$ [36]. Table 2 presents the values of the controller's parameters that are adopted in executing the control algorithm.

Table 2. Controller's parameters.

Parameter	value
c_1	1.25
c_2	1.25
w	0.75
Number of particles	30
Number of iterations	50

4. Simulation Results

The closed-loop response given in Eq. (7) was adopted to calculate the robust controller effort with the PSO technique that was given in Eqs. (8)-(11). The evaluation was conducted through three different parameter values, which are: velocity of moving load, frequency of moving load, and subtended angle.

At the first step, the deflection of the curved beam was calculated by moving a constant force upon it. Figure 5 demonstrates the responses of the curved beam under three different speeds (V = 1, 10, 30, and 50 m/s).

Figure 6 presents the response of the mid-point of the beam when the beam angle was changed as ($\theta = 10^o, 20^o, 30^o,$ and 40^o) with a constant force speed of (V = 10 m/s) and an angular frequency of ($\omega_f = 15$ rad/s). It is apparent that the beam deflection decreases when the angle is reduced due to the high beam stiffness when its curvature increases. When the system is controlled under the same conditions, the controller is capable of depressing the maximum deflection value at ($\theta = 10^o$) by a rate of 98 %. Figure 7 illustrates the deflection value of the controlled system, which is equal to 0.7 mm, and it is a significantly low value compared to the uncontrolled value.

Figure 8 shows the deflection responses of the curved beam under direct load versus the load positions when the following conditions are assumed, ($\theta = 10^o, 20^o, 30^o,$ and 40^o), a constant speed of load ($V = 10$ m/s), and an angular

excited frequency of ($\omega_f = 15$ rad/s). In this figure, a clear trend of decreasing the beam deflection at the load position when the curvature angle decreases, is strong evidence of increasing the beam stiffness. Accordingly, for the same applied conditions with the controller, it is interesting to note that the controller can reduce the deflection beam values as well as change the response configuration to a similar shape at both sides of the beam, as shown in Fig. 9.

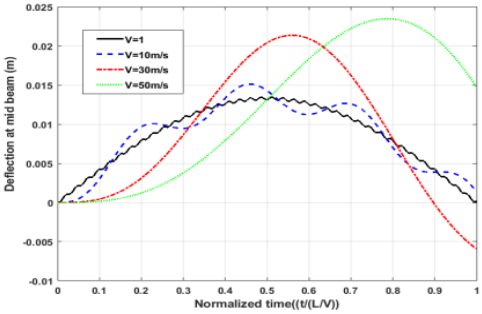

Fig. 5. Deflection at the midpoint versus normalized time ($\theta = 30^o, F_o = 500$ N)

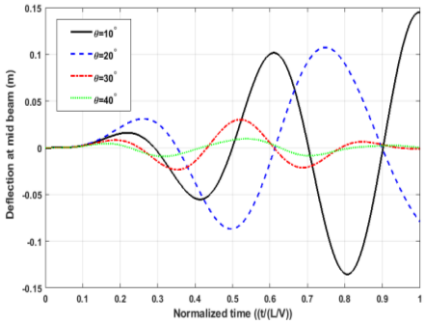

Fig. 6. Deflection at mid curved beam without controller. ($V = 10$ m/s , $\omega_f = 15$ rad/s)

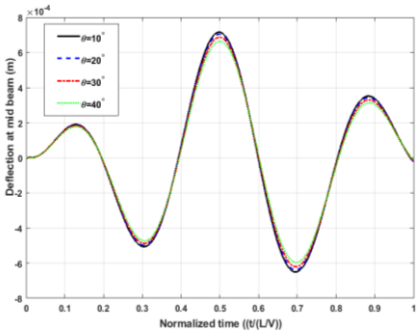

Fig. 7. Deflection at the mid curved beam with controller. ($V = 10$ m/s, $\omega_f = 15$ rad/s).

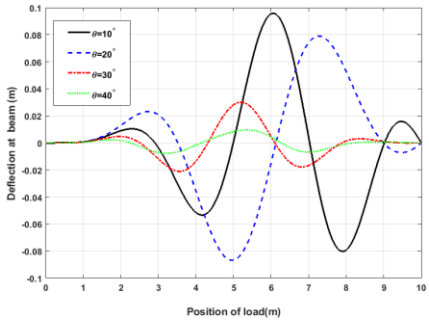

Fig. 8. Deflection of the curved beam under moving load without controller. ($V = 10$ m/s , $\omega_f = 15$ rad/s).

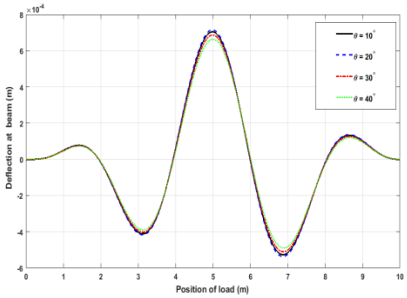

Fig. 9. Deflection of the curved beam under moving load with controller. ($V = 10\,m/s$, $\omega_f = 15$ rad/s).

Figure10 presents the deflection responses of the curved beam at the midpoint versus normalized time when the following conditions are assumed; ($\theta = 30^o$), a different speed of the load ($V = 5, 15, 30$ m/s), and an angular excited frequency of ($\omega_f = 15$ rad/s). It can be noted that the deflections at the mid beam are affected by the interfacing that occurs between the deflections provided by the moving load and the fluctuating load as well. Accordingly, when applying the same conditions for the controlled system, it is interesting to notice that the controller can reduce the beam's deflection values significantly. This occurs at maximum deflection which is obtained when the load speed is (V =15 m/s). The deflection rate of this case reached up to 97.8%, as shown in Fig. 11.

Figure 12 shows the deflection responses of the curved beam versus load positions when the following conditions are assumed, ($\theta = 30^o$), a different speed of the load ($V = 5,15,30$ m/s), and an angular excited frequency of ($\omega_f = 15$ rad/s).

Like the uncurved beam case, the deflections of the curved beam in the current study change continuously with increasing load speed at the load position. In addition, the deflection amplitude tends to move to the right end of the beam when the load speed increases. However, by applying the controller using the same conditions above, the deflection amplitudes are depressed effectively along the beam, as depicted in Fig. 13.

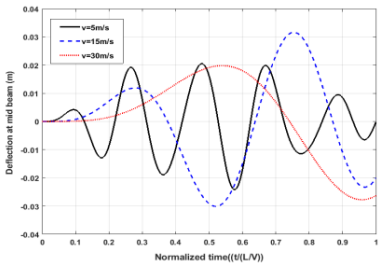

Fig. 10. Deflection at mid curved beam without controller. ($\theta = 30^o, \omega_f = 15$ rad/s).

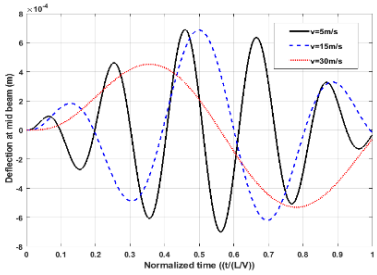

Fig. 11. Deflection at the mid curved beam with controller. ($\theta = 30^o, \omega_f = 15$ rad/s).

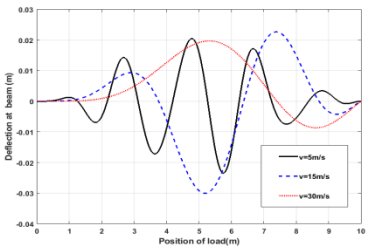

Fig. 12. Deflection of the curved beam under moving load without controller. ($\theta = 30^o, \omega_f = 15$ rad/s).

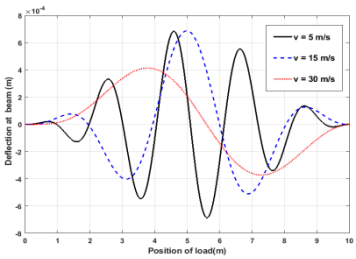

Fig. 13. Deflection of the curved beam under moving load with controller. ($\theta = 30^o, \omega_f = 15$ rad/s).

The responses of the curved beam were tested under different exciting frequencies of ($\omega_f = 5{,}15{,}23 \cdot 9{,}30$ rad/s), with a beam curvature angle of ($\theta = 30^o$) and a load speed of (V=10 m/s). Figure 14 depicts the effect of these frequencies on the beam deflection at the mid. It is clear that when the frequency is (23.9 rad/s), the beam deflection starts to depress as the frequency decreases from that value. What is interesting in using the proposed controller is that the amplitude of the beam vibration was reduced even at the resonant frequency of (ω_f = 23.9 rad/s) with an excellent deflection rate reduction that reached 99.2 %, as shown in Fig. 15. Figures 16 and 17 show the beam deflection responses versus load positions under the same conditions given above without and with the controller, respectively. A clear benefit of the proposed controller is in the preventing and limiting of the beam deflection that could be identified despite a resonance case.

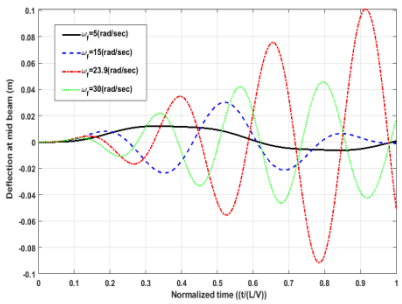

Fig. 14. Deflection at mid curved beam without controller. ($\theta = 30^o$, V = 10 m/s).

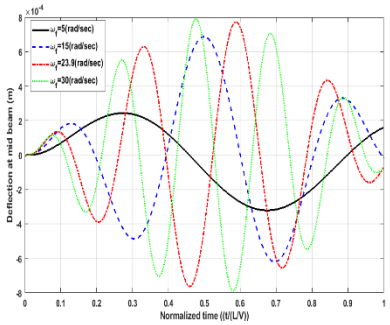

Fig. 15. Deflection at the mid curved beam with controller. ($\theta = 30^o$, V = 10 m/s).

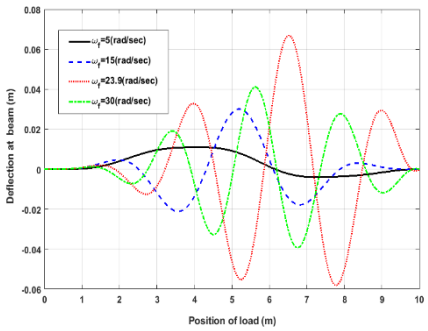

Fig. 16. Deflection of the curved beam under moving load without controller. ($\theta = 30^o$, V = 10 m/s).

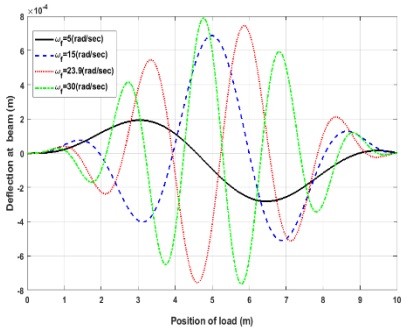

Fig. 17. Deflection of the curved beam under moving load with controller. ($\theta = 30^o$, V = 10 m/s).

Table 3 summarizes the deflections measurements values at the midpoint for the curved beam system and the performances of the PID and the NLNPID schemes that are subjected to different load cases for the normalized duration, in comparison with the values obtained from the non-controlled system. The findings indicate that both schemes have significant results compared to findings of the non-controlled system. It is clear that in the comparison of performances between PID and

NLNPID, the performance on the beam deflection is much less for the NLNPID compared to the PID. Moreover, it can be noticed that the proposed NLNPID controller was able to suppress vibration up to 99 % at the resonance, while the PID controller suppresses vibration up to 44 % only. This shows the high performance of the NLNPID controller. It is interesting to note that the results support the main goal of this study, which is to achieve the depressing of the beam's deflection as much as possible.

Table 3. The midpoint deflections result of the curved beam with and without control.

Different load cases			Without control	PID controller	Reduction rate %	NLNPID Controller	Reduction rate %
ω_f rad/s	V m/s	θ°	m	m		m	
5	10	30	0.0121	0.0045	63.1	3.217e-4	97.3
15	10	30	0.0301	0.013	54.5	6.866e-4	98
23.9	10	30	0.1	0.058	41.1	7.73e-4	99.2
30	10	30	0.042	0.018	56.3	7.89e-4	98.1
15	5	30	0.0241	0.0096	60.1	6.94e-4	97.1
15	15	30	0.0316	0.011	64.5	6.86e-4	97.8
15	30	30	0.0273	0.0112	58.7	5.3e-4	98
15	10	10	0.1075	0.049	53.7	7.15e-4	99.3
15	10	20	0.145	0.061	54.1	7e-4	99.5
15	10	40	0.0096	0.0037	61.3	6.6e-4	93.1
Average Deflection reduction					**56.4**		**97.7**

To realistically prove the controller's action, Fig. 18 shows the response of the control input represented by an actuator force on the beam. The actuation force did not exceed (500 N), which is the maximum amplitude of the moving force on the beam.

It is recognized that when modelling any mechanical system, and whatever the accuracy of that modelling was, uncertainties must be taken into consideration. Therefore, a robust design of the proposed controller is recommended that is capable of dealing with different cases that might be encountered in mechanical systems. In this study, uncertainties are introduced by varying the values of the elastic modulus and the density of the material, where the variation is taken about ± 10% from the mean value, which gives more flexibility to the beam and exposes it to violent vibrations that might be unexpected. The performance of the proposed controller is examined according to these uncertainties. Significant results of the response of the beam deflection at the middle point are obtained. Figure 19 displays the response of the beam's deflection corresponding to reducing the elastic modulus and the density of the material of -10%. The figure shows the effectiveness of the proposed controller by depressing the vibration to 94% against the non-controlled beam.

In this work, the controlled system is considered by the emerging actuator force parallel to the passive components (the damper-spring system). Experimentally, the deflections of the curved beam under different operating conditions are consciously recorded by sensors. Based on the signals obtained by the sensors and the prescribed control strategy, the force in the actuator is modified to attain significant

vibration depressing performance. The functionality of the actuator's action can be produced by many systems such as hydraulic, pneumatic, or electric systems.

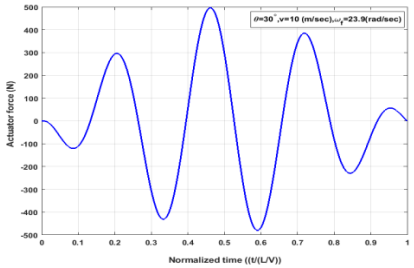

Fig. 18. The control force response with time.

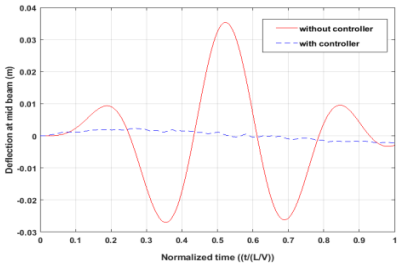

Fig. 19. The control robustness.

5. Conclusions

In this study, the simple mathematical model and the equation of motion for an in-plane curved beam were derived analytically. The derivation was based on simply supported boundary conditions and by adopting the Lagrangian mechanic's theory. The NLNPID controller was proposed for the first stage. Then, the controller was optimized based on the PSO technique. Unlike numerical methods for analysis and modelling, the developed model is easy and compatible with the proposed controller. The closed-loop system was examined by applying three different parameters' values which are: velocity of moving load, frequency of moving load, and subtended angle. According to the simulation results, the following conclusions are obtained;

- The approach has enhanced deflection reduction up to 97.7 % in the case of the adopted NLPID controller for controlling the curved beam system and up to 56.4 % in the case of the PID controller.
- The deflection depressing rate reaches up to 99.2 % for critical conditions (resonance case), which is very hard to obtain for different analyses and control methods.
- Despite the existed uncertainties that were considered in this study, the control system showed a significant rate of reduction of up to 94 %. This is a confirmation of the robustness and stability of the proposed approach.
- The system showed very efficient effort for minimizing the vibrations when subtended angles and load conditions were varied. In addition, it provided smooth and acceptable force action without sharp spikes.
- The study provides insights into practical solutions to curved beam systems. In conclusion, this analysis is expected to show great potentials in engineering applications.

This work has provided promising avenues for future research in the study of the curved beam system, as follows:

- The proposed control objectives and strategies should be applied to other different boundary conditions.

- The effectiveness of the proposed method should be verified by an experimental work for investigation under the proposed control approaches for future works.
- It is suggested that a similar approach can be adopted by taking into consideration the actuator's model and the effects of the time delay.

References

1. Ali, A.A.; and Kareem, H.K. (2020). Numerical modelling of small scale model piles under axial static load. *Journal of Engineering Science and Technology* (*JESTEC*), 15(6), 3528-3546.
2. Ary, A.K.; Prabowo, A.R.; and Imaduddin, F. (2020). Structural assessment of alternative urban vehicle chassis subjected to loading and internal parameters using finite element analysis. *Journal of Engineering Science and Technology*(*JESTEC*), 15(3), 1999-2022.
3. Gebregziabher, H.K.; and Assefa, T. (2021). Simplified full dynamic analysis of a railway tunnel in Ethiopia. *World Journal of Engineering and Technology*, 9(3), 444-457.
4. Asad, J.; and Florea, O. (2020). Numerical aspects of two coupled harmonic oscillators. *Analele Universitatii "Ovidius" Constanta - Seria Matematica*, 28(1), 5-15.
5. Asad, J.; Florea, O.; and Khalilia, H. (2020). Numerical study of the motion of a heavy ball sliding on a rotating wire. *Bulletin of the Transilvania University of Brasov, Series III: Mathematics, Informatics, Physics*, 13(62), No. 1, 33-40.
6. Shanak, H.; Jarrar, R.O.; Khalilia, H.; and Asad, J. (2020). Some features of double pendulum system-numerical and simulation study. *Journal of Theoretical and Applied Mechanics*, 51, 76-91.
7. Narvydas, E.; and Puodziuniene, N. (2020). Curved beam stress analysis using a binary image of the cross-section. *Computer Applications in Engineering Education*, 28(6), 1696-1707.
8. Migliaccio, G.; Ruta, G.; Bennati, S.; and Barsotti, R. (2020). Curved and twisted beam models for aeroelastic analysis of wind turbine blades in large displacement. *In: Carcaterra A., Paolone A., Graziani G.* (*eds*) *Proceedings of XXIV AIMETA Conference* 2019. *AIMETA* 2019. *Lecture Notes in Mechanical Engineering*. Springer, Cham.
9. Kim, N.-I.; and Kim, M.-Y. (2005). Thin-walled curved beam theory based on centroid-shear center formulation. *Journal of Mechanical Science and Technology*, 19, 589-604.
10. Liang, F.; Yang, X.-D.; Bao, R.-D.; and Zhang, W. (2016). Frequency analysis of functionally graded curved pipes conveying fluid. *Advances in Materials Science and Engineering*, Volume 2016 |Article ID 7574216, 9 pages.
11. Michaltsos, G.; Sophianopoulos, D.; and Kounadis, A.N. (1996). The effect of a moving mass and other parameters on the dynamic response of a simply supported beam. *Journal of Sound and Vibration*, 191(3), 357-362.
12. Lee, B.K.; Oh, S.J.; Mo, J.M.; and Lee, T.E. (2008). Out-of-plane free vibrations of curved beams with variable curvature. *Journal of Sound and Vibration*, 318(1), 227-246.

13. Oni, S.T.; and Omolofe, B. (2011). Dynamic response of prestressed rayleigh beam resting on elastic foundation and subjected to masses traveling at varying velocity. *ASME, Journal of Vibration and Acoustics*, 133(4): 041005 (15 pages).
14. Zarfam, R.; Khaloo, A.R.; and Nikkhoo, A. (2013). On the response spectrum of Euler bernoulli beams with a moving mass and horizontal support excitation. *Mechanics Research Communications*, 47, 77-83.
15. Wang, Y.J.; Shi, J.; and Xia,Y. (2012). Dynamic responses of an elastic beam moving over a simple beam using modal superposition method. *Journal of Vibroengineering*, 14(4) , 1824-1832.
16. Bakhtiari, I.; Behrouz, S.J.; and Rahmani, O. (2020). Nonlinear forced vibration of a curved microbeam with a surface-mounted light driven actuator. *Communications in Nonlinear Science and Numerical Simulation*, 91, 105420.
17. Shanmugam, N.E.; Thevendran, V.; Richard Liew, J.Y.; and Tan, L.O. (1995). Experimental study on steel beams curved in plan. *Journal of Structural Engineer*, 121(2), 249-59.
18. Izzet, A.F.; and Mohammed, A.R. (2018). Experimental study on curved composite I-girder bridge subjected to Iraqi live loading for road bridges. *Journal of Engineering Science and Technology* (*JESTEC*), 13(1), 226-241.
19. Boğa, C.; and Onur, S. (2020). Stress analysis of functionally graded beams due to thermal loading. *Journal of Engineering Science and Technology* (*JESTEC*), 15(1), 054-065.
20. Yanze, L.; Ke, Z.; Huaitao, S.; Songhua, L.; and Xiaochen, Z. (2021). Theoretical and experimental analysis of thin-walled curved rectangular box beam under inplane bending. *Scanning*, Volume 2021 |Article ID 8867142, 19 pages.
21. Khot, S.M.; Yelve, N.P.; and Iyer, R. (2008). Active vibration control of cantilever beam by using optimal (LQR) controller. *Proceedings of International Conference on 'Total Engineering, Analysis and Manufacturing Technologies'* (*TEAM Tech* 2008). JN Tata Auditorium, IISc Bangalore, India, 22-24.
22. Khot, S.M.; Yelve, N.P.; Tomar, R.; Desai, S.; and Vittal, S.(2012). Active vibration control of cantilever beam by using PID based output feedback controller. *Journal of Vibration and Control*,18(3), 366-372.
23. Abdelhafez, H.; and Nassar, M. (2016). Effects of time delay on an active vibration control of a forced and self-excited nonlinear beam. *Nonlinear Dynamics*, 86, 137-151.
24. Abiduan, S.H.; Abd Al-Amir, S.H.; and Aboud, W.S. (2018). Vibration control of clamped affected by dynamic load with electromagnetic actuator. *Association of Arab Universities Journal of Engineering Sciences*, 25(1), 170-182.
25. Zhang, T.; and Li, H. (2020). Adaptive modal vibration control for smart flexible beam with two piezoelectric actuators by multivariable self-tuning control. *Journal of Vibration and Control*, 26(7-8), 490-504.
26. Singh, K.; Sharma, S.; Kumar, R.; and Talha, M. (2021). Vibration control of cantilever beam using poling tuned piezoelectric actuator. *Mechanics Based Design of Structures and Machines*, 2(1), 290-307.
27. Kara, A. (2009). *In-plane vibration of curved beam having variable curvature and cross*-sec*tion*. M.Sc. Thesis. School of Engineering and Sciences of İzmir Institute of Technology, İzmir, Turkey.

28. Esen, İ. (2011). Dynamic response of a beam due to an accelerating moving mass using moving finite element approximation. *Mathematical and Computational Applications*, 16(1), 171-182.
29. Yang, Y.-B.; Wu, C.-M.; and Yau, J.-D. (2001). Dynamic response of a horizontally curved beam subjected to vertical and horizontal moving loads. *Journal of Sound and Vibration*, 242(3), 519-537.
30. Mohamed, M.J.; and Hamza, M.K. (2019). Design PID neural network controller for trajectory tracking of differential drive mobile robot based on PSO. *Engineering and Technology Journal*, 37(12A), 574-583.
31. Bahita, M.; and Belarbi, K. (2012). Neural stable adaptive control for a class of nonlinear system without use of a supervisory term in the control law. *Journal of Engineering Science and Technology* (*JESTEC*), 7(1), 97-118.
32. Omatu, S.; Khalid, M.; and Yusof, R. (1996). *Neuro-control and its applications* (1st ed.). London: Springer Ltd.
33. GirirajKumar, S.M.; Jayaraj, D.; and Kishan, A.P. (2010). PSO based tuning of a PID controller for a high performance drilling machine. *International Journal of Computer Applications*, 1(19), 12-18.
34. Talukder, S. (2011). *Mathematical modeling and applications of particle swarm optimization*. M.Sc. Thesis. School of Engineering, Blekinge Institute of Technology, Karlskrona, Sweden.
35. Al-Araji, A.; and Rasheed, L.T. (2016). Design of a nonlinear fractional order PID neural controller for mobile robot based on particle swarm optimization. *Engineering & Technology Journal*, 34(12), 2318-2333.
36. Kaipa, K.N.; and Ghose, D. (2017). *Glowworm swarm optimization: Theory, algorithms, and application.* (1st ed.). Springer.